sociedade & natureza

DOI: 10.14393/SN-v32-2020-52769
Received: 17 February 2020 | Accepted: 02 June 2020

Precipitation in northern Amazonia: Spatial distribution in Roraima, Brazil

Paulo Eduardo Barni[1]
Reinaldo Imbrozio Barbosa[2]
Haron Abrahim Magalhães Xaud[3]
Maristela Ramalho Xaud[4]
Philip Martin Fearnside[5]

Keywords
Climate. Rainfall
Ordinary Kriging
Spatial modeling

Abstract
Rainfall is one of the most important variables for studies of biological processes. In the Amazon, studies of the spatial and temporal distribution of rainfall have been used as an analysis tool in regional planning aimed at the conservation of different ecosystems. This is exemplified by the construction of agricultural calendars and by controlled burning to prevent the fires that are used to clear fields and maintain pastures from escaping from control and turning into large forest fires in years of severe drought. Our study aimed to model the spatial distribution of rainfall in Brazil's state of Roraima (1998-2018) at monthly and annual scales based on orbital data from two products available on the world-wide web (TRMM and WORLDCLIM). Ordinary kriging was adopted as a method for geostatistical modeling of precipitation considering the 59 meteorological stations located in the study area. Roraima has two well-defined climatic seasons in the year, but these seasons are inverted between the portions of the state in the northern and southern hemispheres. On average, 63.5% of the precipitation in the *Af* (without dry season) climate area falls between March and August, with a peak in May, while in both the *Am* (monsoon) and *Aw* (with dry winter) climates rainfall is concentrated between April and September (73% in *Am* and 82.3% in *Aw*), with the peak in June. Between 1998 and 2018 the average annual precipitation was 1925 ± 339.7 mm, regardless of the hemispheric location. Extreme climatic events have a dramatic effect on regional rainfall, where El Niño years (long droughts) are characterized as drier periods with higher risks of forest fires, while in La Niña years (wetter periods) there are higher probabilities of heavy rains associated with long periods of flooding.

[1] Universidade Estadual de Roraima – UERR, Campus Rorainópolis. Avenida Senador Hélio Campos, S/N. 69373-000 Rorainópolis, RR. pbarni@uerr.edu.br
[2] Instituto Nacional de Pesquisas da Amazônia - INPA, Rua Coronel Pinto, 315. 69301-150 Boa Vista, RR. reinaldo@inpa.gov.br
[3] Empresa Brasileira de Pesquisa Agropecuária – Embrapa/RR. Rodovia BR 174, Km 8, Distrito Industrial. 69301-970 Boa Vista, RR. haronxaud@gmail.com
[4] Empresa Brasileira de Pesquisa Agropecuária – Embrapa/RR. Rodovia BR 174, Km 8, Distrito Industrial. 69301-970 Boa Vista, RR. marisxaud@gmail.com
[5] Instituto Nacional de Pesquisas da Amazônia - INPA, Av. André Araújo, 2936. 69067-375 Manaus, AM. pmfearn@inpa.gov.br

INTRODUCTION

Rainfall is one of the most important variables for biological processes and for forest conservation (FEARNSIDE, 2008; BRANDO et al., 2014) and can be used as an important analysis tool in investigations that associate droughts with deforestation and forest fires in the Amazon (ARAGÃO et al., 2007; BRANDO et al., 2020). Understanding the spatial distribution of rainfall also has a strong link to regional planning actions associated with drafting agricultural calendars and programming controlled burning. These actions are taken to prevent fires derived from agricultural burning from escaping from control and turning into large-scale forest fires in years of severe drought (BARBOSA; FEARNSIDE, 1999; ALENCAR et al., 2006; ARAGÃO; SHIMABUKURO, 2010; XAUD et al., 2013; BARNI et al., 2015a; FONSECA et al., 2017). Despite the recent advances represented by the spatial expansion of the terrestrial data-collection network and the support of various public institutions and indigenous communities, riverside communities and farmers (http://www.snirh.gov.br/hidrotelemetria/serieHistorica.aspx), the Amazon still has areas that are difficult to reach and that lack any historical data series provided by conventional means (ALVARES et al., 2014). The most data-poor area is in the far north of Amazonia, especially in the state of Roraima.

An example of this lack of information in Roraima is provided by the fact that, until recently, Roraima's state the government only used the rainfall frequency data obtained from the INMET (National Institute of Meteorology) weather station in Boa Vista to characterize the climate of the entire state (CASTRO; MIRANDA, 2016; SILVA et al., 2015). Another example is a document prepared by the MDA (Ministry of Agrarian Development), an agency under the Presidency of the Republic, which characterizes the climate of the municipalities in the state's Southern Region (BARNI et al., 2012, 2015b), which are classically defined as rainy tropical monsoon (*Am*), as "*Aw*," which is a climate type characteristic of savanna areas (MDA, 2010, pp. 35-57).

This situation ends up damaging the socio-economic-environmental planning of the state of Roraima, inhibiting the development of science and technology by depriving undergraduate and graduate students of high-quality science-based meteorological information. For example, creating efficient public policies to fight forest fires in Roraima involves the elaboration of calendars for agriculture and for controlled burning, which require high-quality meteorological information that is specific to each of the state's climatic regions.

Although important advances have been made in policies for fighting forest fires in the state of Roraima in recent years (e.g., FONSECA et al., 2017; CAMMELLI; ANGELSEN, 2019), there is a continuous need to develop and perfect a self-regulated or automated system that assists in decision making at the regional level. One such local system is promoted by the Committee for Preventing and Fighting Forest Fires, which was started in 1999 following the great Roraima fire of 1997/1998 (BARBOSA et al., 2003). Unlike its initial stages, this program is now more fully functional thanks to the participation of communities affected by forest fires. The committee has the purpose ensuring that the program functions fully, not only protecting private property but also the common good represented by the forest's environmental services (e.g., FEARNSIDE, 2013; MEDINA et al., 2015; FONSECA-MORELLO et al., 2017). As an additional contribution, the TERRAMZ project (Shared Knowledge for Local Territorial Management in the Amazon), which is being implemented by an EMBRAPA/BNDES/Amazon Fund partnership, has been working on building participatory mechanisms for preventing, monitoring and controlling forest degradation by forest fires, seeking to advance in creating (semi) automated fire-monitoring and alert systems (TERRAMZ, 2020).

These promising initiatives are based on the understanding that efforts to avoid the loss of the forest's biodiversity and environmental services are critical. These efforts must move towards eliminating the sources of ignition created by deforestation and the use of fire in maintaining pastures and agricultural fields; in addition, understory forest fires should be suppressed when they occur (MORTON et al. 2013; SILVA et al., 2018; STAAL et al., 2020).

Modeling the spatial distribution of precipitation (or other biophysical variables) over the surface of a region, which can serve as a basis for creating realistic scenarios and assist in decision making, can be a viable alternative in the face of limited information from a network of conventional rain gauges (e.g., FONSECA et al., 2017; BRANDO et al., 2020). In addition, the current advancement in information technology has allowed substantial improvement in the degree of certainty of data obtained remotely

(PRAKASH et al., 2016), thus facilitating the application of spatial modeling based on geostatistical interpolation methods (BACCINI et al., 2012; AVITABILE et al., 2016; BARNI et al., 2016).

Concomitant with the technological advances that took place in this period, geoprocessing products were developed on a worldwide scale (WORLDCLIM) using biophysical variables such as air temperature and rainfall (HUFFMAN et al., 1997; HIJMANS et al., 2005; FICK; HIJMANS, 2017). These developments also helped to boost scientific research at the local/regional level (ALVARES et al., 2014; YANG et al., 2017). In this context, the database that is generated from measurements by the Tropical Precipitation Measurement Satellite (TRMM), compiled by the National Aeronautics and Space Administration (NASA, USA) in partnership with the Japanese Space Agency (JAXA) for studies of precipitation in the tropics (PASSOW, 2010; MACRITCHIE, 2015), plays an important role worldwide (CHEN; LI, 2016; YANG et al., 2017).

On the other hand, considering online platforms that provide remote-sensing products for climate studies in Brazil, we can mention the Mineral Resources Research Company (CPRM) (https://www.cprm.gov.br/publique/Hidrologia/MAP-e-Publicacoes/Atlas-Pluviometrico-do-Brasil-1351.html), the National Water Agency (ANA) (https://www.ana.gov.br/panorama-das-aguas/divisoes-hidrograficas), INMET (http://www.inmet.gov.br/portal/) and the Center for Weather Forecasting and Climate Studies (CPTEC) (https://www.cptec.inpe.br/). These agencies provide an excellent service to the Brazilian scientific community within the area of specialization of each agency (CPRM: maps of climatological normals; ANA: management and data from rain gauges, and INMET and CEPTEC: maps and climate analyses).

The present study therefore had as its objective the application of geostatistical models to the spatial distribution of precipitation in Roraima (1998-2018) at monthly and annual scales based on orbital data from the TRMM and WORLDCLIM products that are available on the world-wide web. Based on spatial modeling, this study aims to build a reference map for rainfall frequency in the state of Roraima and neighboring areas.

MATERIAL AND METHODS

Study area

Although our aim for generating the spatial distribution of rainfall is restricted to the state of Roraima (224,303.1 km²: IBGE, 2020), modeling this distribution required information on an area of 687,072 km² (816 km × 842 km) that covered parts of the Brazilian states of Amazonas and Pará, in addition to part of southern Venezuela and western Guyana (Map 1). This procedure aims to avoid or minimize distortions caused by the edge effect, which are common in the application of geostatistical interpolation techniques (BARNI et al., 2016).

Spatial modeling

Geostatistical modeling of the spatial and temporal distribution of precipitation in the state of Roraima was carried out by making precipitation maps from two remote-sensing products. The first was TRMM 3B43 (http://trmm.gsfc.nasa.gov/), providing maps in the Hierarchical Data Format (HDF, a standardized data-storage file format) at a spatial resolution of 0.25 degrees (~27.75 km; 1 - ~111 km). The second product was WORLDCLIM (http://www.worldclim.org/current), with maps in raster format (a grid of cells) at a spatial resolution of 10 minutes or 0.16666668 degrees (~18.5 km).

In the case of the TRMM 3B43 product, the monthly maps were obtained with precipitation values in mm hour^{-1} for the years from 1998 to 2018. The TRMM 3B43 database is calibrated from rain-gauge data (MACRITCHIE, 2015).

Considering WORLDCLIM, the values were obtained from maps of climatological averages for each month (1960 to 1990) in mm month^{-1}. The precipitation values of the WORLDCLIM maps were obtained for approximately the same coordinates as the TRMM 3B43 data in order to allow comparisons of the data after spatial modeling.

The WORLDCLIM dataset was initially produced by Hijmans et al. (2005) using rainfall data from a global network of rain gauges covering the 1950–2000 period. The maps were produced at a spatial resolution of 30 arc s^{-1} (~1 km) by geostatistical interpolation techniques using latitude, longitude and altitude as independent variables.

After obtaining the two databases for the study area, these were converted to the vector (shapefile) format. The vector files were then randomly subdivided into two separate datasets, randomly considering the entire sampling quadrant in two distinct sets of data. The first set was used for the mapping and the second for

the cross-validation (the reserve or test set). Mapping was performed using the ordinary kriging geostatistical method. Ordinary kriging is a robust geostatistical interpolation technique that is easy to apply and facilitates interpretation of results (CAMBARDELLA et al., 1994; BELLO-PINEDA; HERNÁNDES-STEFANONI, 2007; BOHLING, 2005; ALVARES et al., 2011; 2014; BARNI et al., 2016). This resulted in a mean precipitation map for each month for the entire study area with 500-m spatial resolution equivalent to a pixel area of 25 ha. A semivariogram was modeled separately for each month, in which the parameters observed in each model were the "nugget" (random error that is intrinsic to the structure and spatial distribution of the data), the "range" (a measure indicating the magnitudes of values for which the model controls the estimates) and the "sill" (the threshold or limit after which the modeled values become random) (e.g., ALVAREZ et al., 2011, 2014; BARNI et al., 2016). All models executed during the kriging of the points were exponential, both for the TRMM and for the WORLDCLIM datasets. The eight closest neighbors (minimum of 4) were used to estimate the value for precipitation at each unsampled location. As a way of evaluating the spatial dependence (SD) of the values of the precipitation variable calculated in each theoretical model, the relationship between the nugget effect and the sill was used, with this index expressed as a percentage; the lower the value of this index, the greater the SD% (CAMBARDELLA et al., 1994).

Map 1 - Study area. The curved lines over Roraima subdivide the area into three climate types: *Af* (equatorial forest climate), *Am* (monsoon climate) and *Aw* (savanna climate) in accord with the Köppen classification (BARBOSA, 1997; ALVARES et al., 2014).

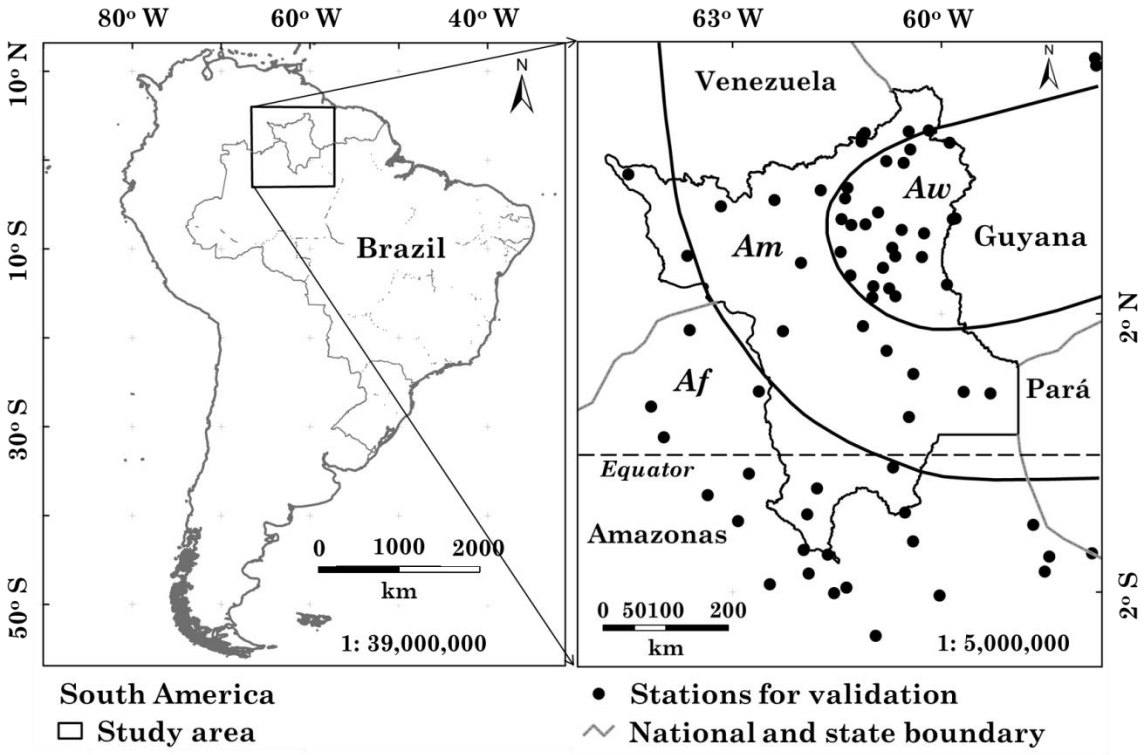

Organized by the authors, 2020.

After making each monthly precipitation map for the entire study area, a monthly precipitation map was extracted that covered only the area within the boundaries of the state of Roraima. Annual precipitation maps were also generated using only TRMM 3B43 data. For the WORLDCLIM data, it was only possible to represent an "average" year, summing the monthly averages to compose the annual precipitation. Manipulating the database and the application of geostatistical techniques, including validation, were performed in a geographical information system (GIS) using Quantum Gis (QGis Desktop 2.18.15) free software (https://www.qgis.org/). The maps were produced from planar coordinates in the Universal Transverse Mercator (UTM) projection, zone 20 north, in the WGS 1984

datum.

Independent cross-validation

Cross-validation was performed from the collection of values estimated by modeling at the point locations (geographical coordinates) that were reserved for validation by comparing these (predicted) values with the values observed in the reserve (test) dataset. To evaluate the parameter values obtained in this process (mean, standard error, standard deviation and coefficient of determination or R^2), statistical analyses were used (simple regression analysis and t test) comparing the predicted values estimated by the model with the observed values in the test dataset. All analyses were performed using R 3.6 free software (R CORE TEAM, 2019) considering the 95% level of statistical confidence (type I error: $\alpha = 0.05$).

The independent validation of the mappings consisted of comparing the precipitation values (mm month^{-1}) of the 59 meteorological stations with the values (maps) estimated by the models obtained for the same geographical coordinates considering the three climate types in the state: *Af* (n = 18), *Am* (n = 16) and *Aw* (n = 25). Evaluation of the parameter values obtained was based on Pearson's correlation coefficients (r) (DANCEY; REIDY, 2006; FIGUEIREDO-FILHO; SILVA JR., 2009) and the statistical significance of the analysis of variance (ANOVA). However, in evaluating the maps of annual means, the annual values of the 59 stations were used without considering the climate types, assuming that this would be a mixture, or a combination of the climatic performance distributed over the period.

The database with 59 meteorological stations uses information collected by Barbosa (1997) from multiple government agencies in Brazil (e.g., ANA, INMET, IBAMA, SINDA/INPE and EMBRAPA), representing 56 stations, in addition to two from Venezuela (Weatherbase) and one from Guyana (Weatherbase) (Flowchart 1). The number of months for each station used for validation ranged from 17 (June 1988 to October 1989) at Apiaú in the municipality of Mucajaí, to 1052 months (January 1910 to December 2011) at Boa Vista. The average data-series length was 213.3 months (~ 18 years), considering all 59 rainfall stations.

Flowchart 1 - Steps required for independent validation of the mappings.

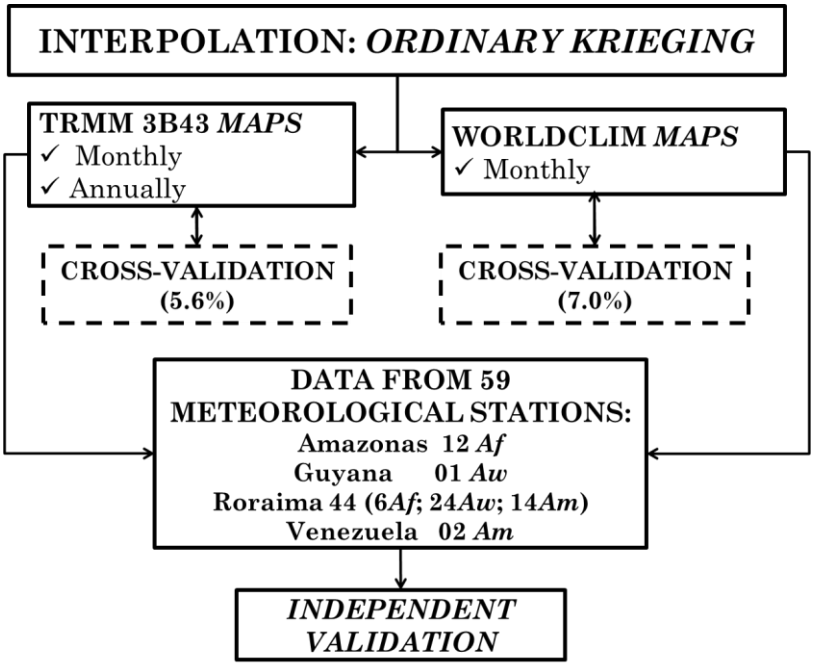

Organized by the authors, 2020.

RESULTS AND DISCUSSION

In general, modeling the spatial distribution of precipitation in the state of Roraima using data from TRMM and WORLDCLIM produced good results. This is shown by the parameters evaluated below.

Considering the semivariograms modeled based on the TRMM data, the months of February, June and November did not have a nugget effect, indicating that these values

showed little or no random error within the limits of the range. The months of May (51.0) and April (43.8) had the highest nugget-effect values, and, theoretically, the models for these months had the highest numbers of random errors (Graph 1A).

Considering the modeling of the semivariogram based on WORLDCLIM data, unlike the results from TRMM, every month showed the nugget effect. The months of May (69.5) and June (63.9) had the highest nugget-effect values and, theoretically, the models for these months had the highest numbers of random errors. The lowest nugget-effect value (5.8) was for February (Graph 1B).

Graph 1 - Semivariogram models of monthly precipitation means for Roraima obtained from the TRMM 3B43 product (A) and from WORLDCLIM data (B). Note: the curves are ordered from the highest to the lowest sill value for each modeled month.

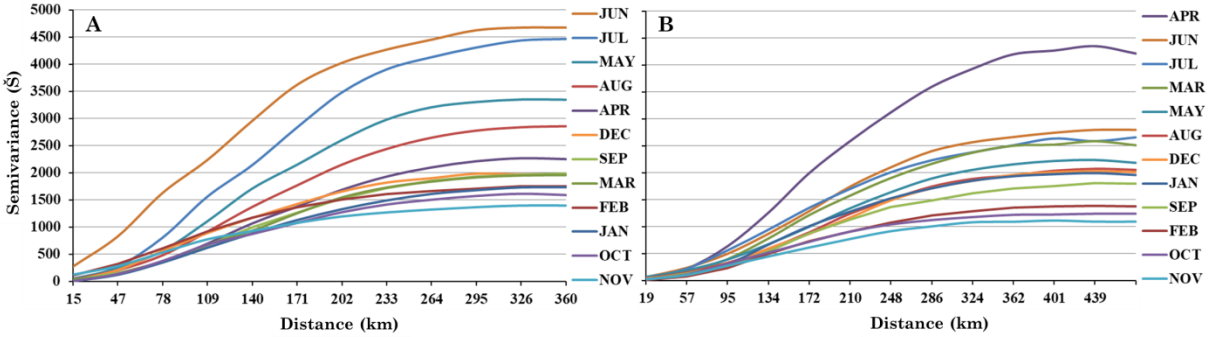

Organized by the authors, 2020.

The mean distance found from the range, considering the geostatistical models using the TRMM 3B43 data, was 275.2 km, while the mean distance was 287.6 km for the semivariograms based on WORLDCLIM data. The WORLDCLIM the mean distance value was only 4.5% higher than the mean distance obtained from the TRMM data. Beyond this limit the modeled results become random (Table 1).

These results indicate that the data, both from TRMM and WORLDCLIM, were well structured due to the regularity of the grid of points. The low values obtained for the nugget effect and the sill indicate a strong spatial dependence (DE) of the modeled random variable (CAMBARDELLA et al., 1994), which is desirable (MELLO; OLIVEIRA, 2016).

Table 1 - Parameters used in modeling of the semivariogram with ordinary kriging based on monthly precipitation from the TRMM 3B43 and WORLDCLIM products. SD= spatial dependence.

	TRMM 3B43				WORLDCLIM			
Month	**Nugget effect**	**Range (km)**	**Sill**	***SD%***	**Nugget effect**	**Range (km)**	**Sill**	***SD%***
JAN	4.7	274.6	1,775.3	0.27	14.3	326.9	2,004.1	0.71
FEB	0.0	306.0	1,761.2	0.00	5.8	328.2	1,404.1	0.41
MAR	36.4	287.3	1,963.9	1.86	17.8	371.9	2,593.7	0.69
APR	43.8	270.2	2,273.5	1.93	47.4	373.4	4,337.2	1.09
MAY	51.0	246.6	3,362.4	1.52	69.5	250.0	2,205.3	3.15
JUN	0.0	300.0	4,771.4	0.00	63.9	243.5	2,764.5	2.31
JUL	20.9	294.3	4,533.5	0.46	51.2	276.6	2,624.1	1.95
AUG	41.0	274.8	2,894.5	1.42	42.4	248.2	2,055.1	2.06
SEPT	34.5	264.6	1,987.9	1.74	24.4	273.1	1,808.1	1.35
OCT	5.1	281.2	1,615.1	0.31	22.5	224.2	1,226.9	1.83
NOV	0.0	264.1	1,417.5	0.00	23.3	239.2	1,111.3	2.09
DEC	14.0	239.2	2,012.3	0.69	39.5	296.4	2,028.1	1.95

According to the monthly precipitation maps modeled from both TRMM 3B43 and WORLDCLIM data, the central part of the state from north to south and the east-central part of the state were the areas that showed the greatest oscillations in precipitation over the course of the year (Figures 1 and 2). These disturbances are probably related to the monsoon climate (*Am*), which influences rainfall in the state, especially in La Niña years (GRIMM, 2003).

Figure 1 - Distribution of mean monthly rainfall in Roraima using TRMM 3B43 data.

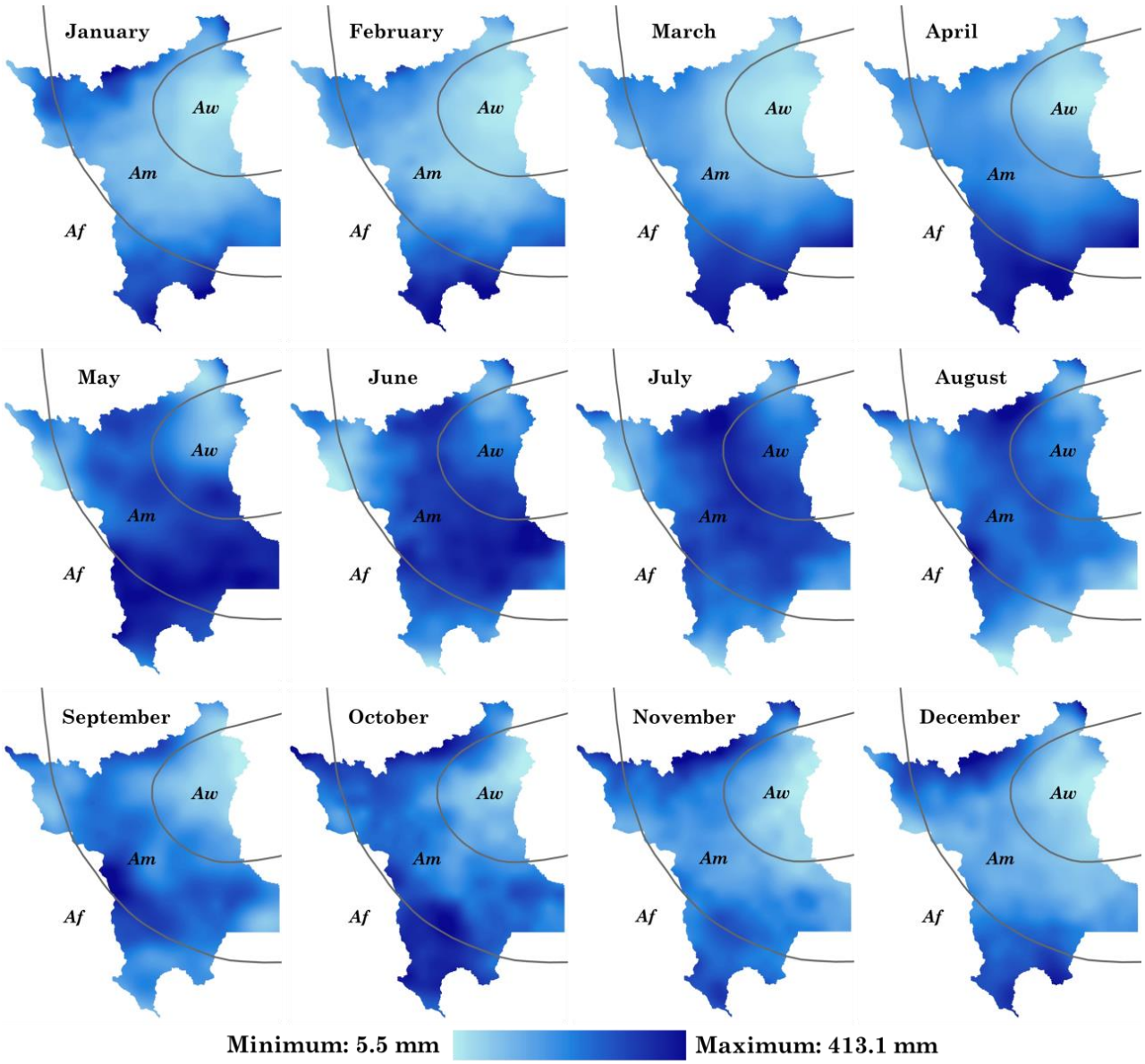

Organized by the authors, 2020.

The area corresponding to the savannas of Roraima, in the northeastern portion of the state, was correctly characterized by both mappings. This area is characterized by low rainfall throughout the year when compared to rainfall over forest areas, and it represents the *Aw* climate (BARBOSA, 1997).

On the other hand, the areas with the highest rainfall (south, southeast, southwest and far north) are characterized by forests and have large stocks of biomass (BARNI et al., 2016). For example, in the southern region, which is close to the equator, the equatorial climate (*Af*) is characterized by torrential rains in the rainy season, and even in the months with lower mean rainfall the monthly precipitation remains between 100 and 150 mm.

Between the *Aw* and *Af* climate areas is an area with the monsoon climate (*Am*). This climate type occurs in a strip covering the south-

central and northwest portions of the state. The *Am* climate type may be related to the climatic inversion that is seen in early September, when the rains start to decrease in the northern part of Roraima, but in the southern hemisphere the rainy season is just beginning (GRIMM, 2003). The climatic inversion coincides with the return of the Intertropical Convergence Zone (ITCZ) to the region close to equator after the end of the northern-hemisphere summer (e.g., WU et al., 2019).

Figure 2 - Distribution of mean monthly rainfall in Roraima from WORLDCLIM data.

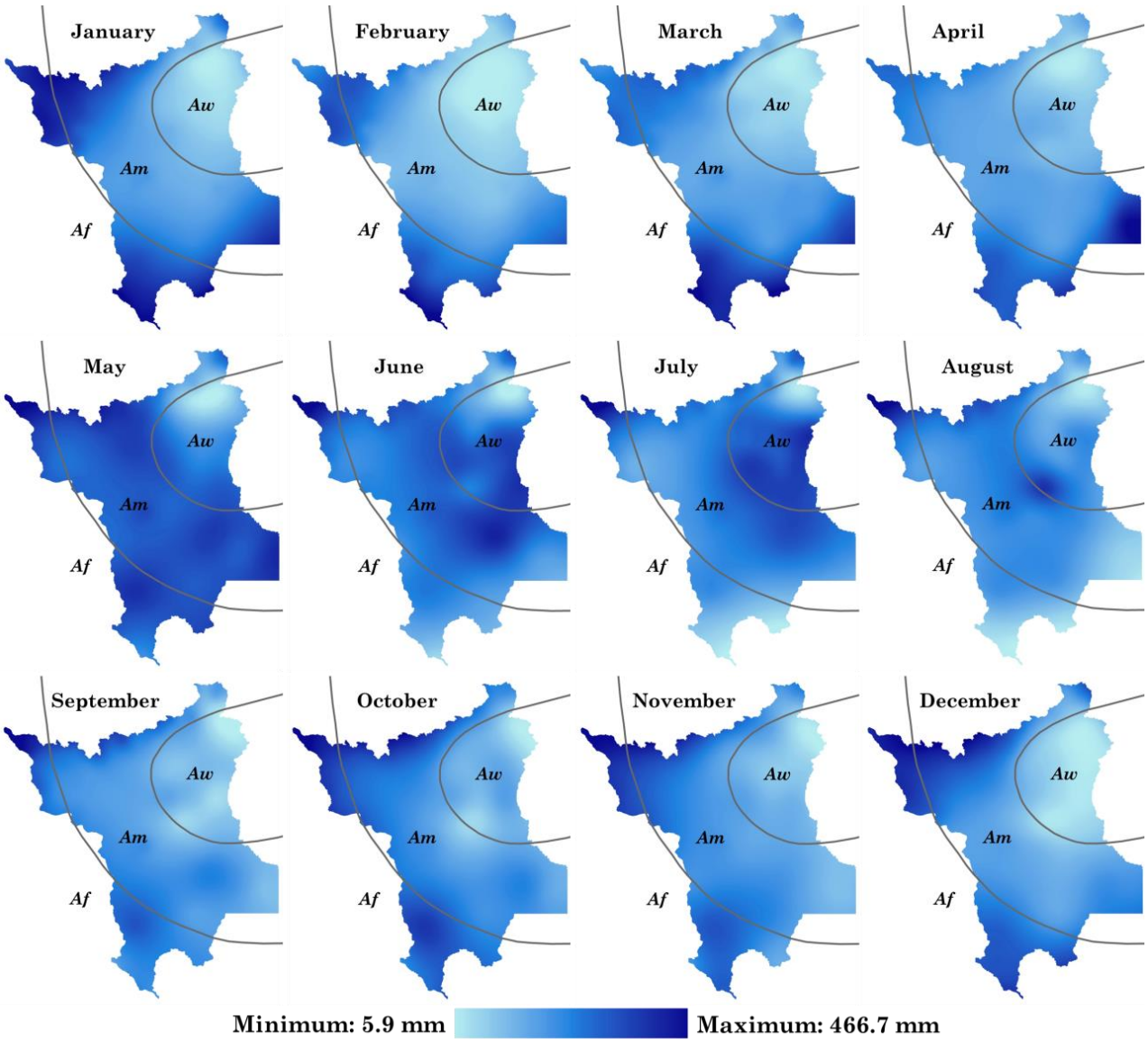

Organized by the authors, 2020.

Tables 2 and 3 show the results of the cross-validation performed with the TRMM 3B43 and WORLDCLIM test databases, respectively. Considering the two analyses, the lowest coefficients of determination were in May, with adjusted R^2 = 0.9745 calculated from TRMM 3B43data and adjusted R^2 = 0.9256 from WORLDCLIM data. On the other hand, the highest values of adjusted R^2 were in June (0.9963) for TRMM 3B43 and February (0.9961) for WORLDCLIM.

Table 2 - Results of cross-validation between the observed values (Mean_O) from TRMM 3B43 and those predicted (Mean_P) by ordinary kriging at 75 reserved points (5.6%).

	Regression analysis					t test		
	Mean_O	**Mean_P**	**Std. dev.**	**$R^2_{Adj.}$**	***p***	**Std. dev.**	**%**	***p***
JAN	154.7	155.1	6.1423	0.9941	<0.0000	80.1	51.8	0.9754
FEB	162.7	162.5	6.7872	0.9942	<0.0000	88.8	54.6	0.9903
MAR	213.6	214.7	8.3671	0.9948	<0.0000	115.5	54.1	0.9544
APR	272.4	272.9	7.7462	0.9864	<0.0000	66.2	24.3	0.9633
MAY	342.2	340.9	10.1960	0.9745	<0.0000	64.3	18.8	0.9056
JUN	281.8	281.9	6.5359	0.9963	<0.0000	108.6	38.5	0.9939
JUL	249.9	250.3	7.4968	0.9961	<0.0000	121.0	48.4	0.9823
AUG	193.1	193.0	7.1944	0.9963	<0.0000	119.5	61.9	0.9951
SEPT	137.2	138.5	7.9510	0.9908	<0.0000	83.7	61.0	0.9200
OCT	134.1	132.9	7.5358	0.9866	<0.0000	65.9	49.2	0.9149
NOV	139.4	139.2	7.5983	0.9847	<0.0000	62.2	44.6	0.9852
DEC	155.5	155.3	7.3675	0.9885	<0.0000	68.7	44.2	0.9885

Table 3 - Results of cross-validation between the observed values (Mean_O) from WORLDCLIM and those predicted (Mean_P) by ordinary kriging at 124 reserved points (7.0%).

	Regression analysis					T test		
	Mean_O	**Mean_P**	**Std. dev.**	**$R^2_{Adj.}$**	***p***	**Std. dev.**	**%**	***p***
JAN	168.3	168.1	7.6683	0.9914	<0.0000	83.1	49.4	0.9857
FEB	155.4	155.7	4.9875	0.9961	<0.0000	80.3	51.7	0.9753
MAR	204.1	204.2	7.1710	0.9939	<0.0000	91.9	45.0	0.9942
APR	253.7	253.7	8.9530	0.9877	<0.0000	81.2	32.0	0.9991
MAY	314.2	312.7	14.7359	0.9256	<0.0000	55.2	17.6	0.8376
JUN	267.5	265.9	13.9233	0.9716	<0.0000	84.8	31.7	0.8829
JUL	221.3	220.3	12.5603	0.9779	<0.0000	85.6	38.7	0.9299
AUG	182.0	181.0	8.2018	0.9899	<0.0000	83.0	45.6	0.9270
SEPT	134.5	133.6	6.7628	0.9887	<0.0000	64.6	48.0	0.9129
OCT	129.2	128.7	5.0614	0.9916	<0.0000	55.4	42.9	0.9483
NOV	134.2	133.5	7.3878	0.9772	<0.0000	49.2	36.7	0.9120
DEC	156.3	155.8	9.9103	0.9758	<0.0000	64.3	41.2	0.9590

Independent validation

Independent validation using the precipitation in the regions with the different climate types indicated a strong correlation between the observed values and the values estimated by the models (Table 4). According to the analysis of variance (p = 0.4606), there was no significant difference at the 95% level of statistical confidence between the values observed at the meteorological stations and the values estimated by the models for the same geographical coordinates.

The highest rainfall values for *Af* were recorded from March to August, regardless of the model, with the highest peak in May. The *Am* and *Aw* climates had the highest precipitation peak in June, with the high-rainfall months extending from April to September. The comparison (ANOVA) of observed and estimated monthly means between climate types (Graphs 2A, 2B and 2C) and within climate types (Graphs 2D, 2E and 2F) did not show significant difference at the 95% level of statistical confidence.

Table 4 - Pearson's correlation analysis (r) relating the values observed at the 59 stations with the values estimated by the models at the same geographical coordinates. The climate types (*Af, Am* and *Aw*) followed by the letters S, T and W indicate the values observed at the stations (S) and the values predicted by TRMM 3B43 (T) and WORLDCLIM (W). Values in bold indicate a strong correlation (r > 0.7000) between the observed and predicted values within each climate type.

	Af_S	***Af_T***	***Af_W***	***Am_S***	***Am_T***	***Am_W***	***Aw_S***	***Aw_T***	***Aw_W***
Af_S	1.0000								
Af_T	**0.9865**	1.0000							
Af_W	**0.9955**	0.9916	1.0000						
Am_S	0.7711	0.7585	0.7511	1.0000					
Am_T	0.7989	0.7897	0.7805	**0.9972**	1.0000				
Am_W	0.7862	0.7705	0.7674	**0.9953**	0.9951	1.0000			
Aw_S	0.7253	0.7151	0.7041	0.9969	0.9898	0.9903	1.0000		
Aw_T	0.7275	0.7250	0.7107	0.9956	0.9918	0.9896	**0.9975**	1.0000	
Aw_W	0.6737	0.6654	0.6530	0.9844	0.9735	0.9815	**0.9935**	0.9895	1.0000

Graph 2 - Average monthly rainfall observed and estimated at the locations of the meteorological stations considering the three climatic types: *Af* (n = 18), *Am* (n = 16) and *Aw* (n = 25). Frequency of monthly precipitation of the three climatic types at the meteorological stations (A: S), TRMM (B: T) and WORLDCLIM (C: W). Panels (D), (E) and (F) present the frequency of monthly precipitation according to the climate types for (D) values observed at the meteorological stations, (E) values modeled from TRMM and (F) values modeled from WORLDCLIM.

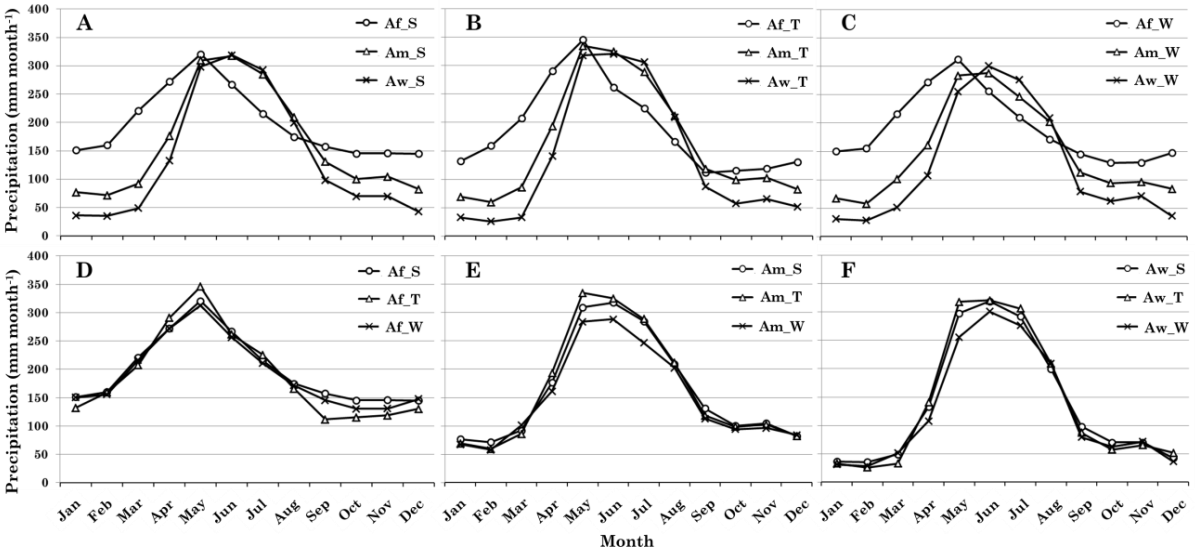

Organized by the authors, 2020.

There were no significant differences (ANOVA: p = 0.2526) between the mean value (1951.1 mm) observed at the 59 meteorological stations and the values of an average year estimated from the TRMM 3B43 data (1925.2 mm) and of an average year estimated from the WORLDCLIM data (1831.5 mm). It can be seen from Graph 3 that the observed data at the meteorological stations had the greatest amplitude while the TRMM 3B43 data had the smallest amplitude among the three databases we compared. This behavior is due to the origin of the TRMM 3B43 data, which are derived from reanalysis (PRAKASH et al., 2016; WOLFF, et al., 2005), thus significantly reducing errors and approximating the values around the mean, while station data are subject to natural stochastic or random rainfall variations. The same can be inferred from the WORLDCLIM data, although this database uses different methods to estimate the values at the sampled points.

From the TRMM 3B43 data it was possible to generate the spatial distribution of annual precipitation (n = 21) for the state of Roraima and surrounding areas. It is interesting to note

that annual rainfall follows a pattern of alternating wet periods of four to five years and dry periods of two to three years. This pattern apparently coincides with the occurrence of El Niño and La Niña years, which have a great influence on the rainfall regime of this state (SILVA et al., 2015) and in Amazonia as a whole (Figure 3).

Graph 3 - Observed annual values ("Stations") and the values predicted or modeled from TRMM ("TRMM 3B43") and WORLDCLIM ("WCLIM") at the 59 meteorological stations in the study area. The vertical bars indicate the extreme quartiles of the samples (first and fourth, respectively). The central lines represent the means and the ends of the boxes delimit the beginning of the second and the end of the third quartile, respectively. The same lower-case letters indicate that there is no significant difference between the means at the 99% level of statistical confidence (α = 0.01).

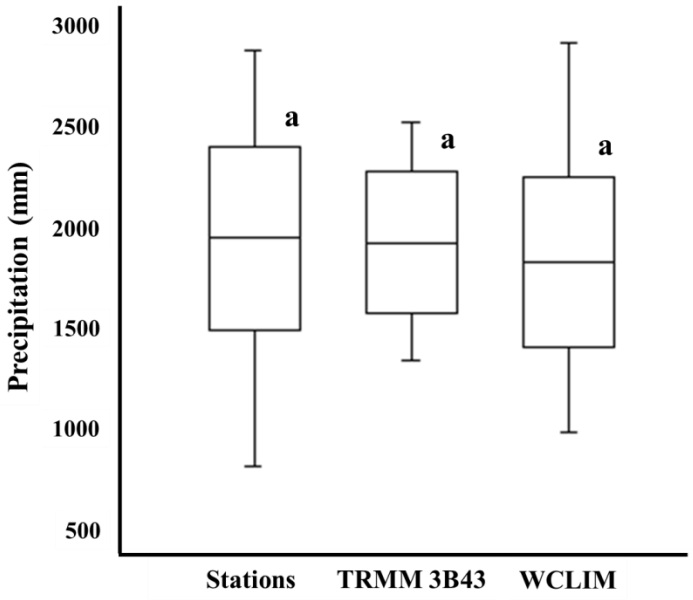

Organized by the authors, 2020.

Between 1998 and 2018, 10 years were recorded with rainfall above the mean of 1925.2 ± 339.7 mm (+1.0 standard deviation) and 10 years below the average (-1.0 standard deviation) for the period, while the year 2004 practically coincided with the mean rainfall value of 1940.3 mm (Graph 4). Despite the heavy rainfall recorded in 2006 and 2007, these years were classified as "weak" El Niño years (SILVA et al., 2015).

On the other hand, the years 2001, 2009, 2014 and 2015 showed anomalously low precipitation, raining one standard deviation below the mean for the period. These years were marked by severe droughts in the state.

It is important to highlight that an annual analysis impedes a better evaluation of the dry periods (from September of one year to March of the following year) and consequently of the influence of climatic phenomena in Roraima (e.g., MARENGO, 1992; GRIMM, 2003). For example, the interval that started in October-November 2015 and ended in early April 2016 was characterized by the influence of one of the most severe El Niños ever recorded in the Amazon (FONSECA et al., 2017; SILVA JR et al., 2019). This El Niño was considered to be even stronger than that of 1997-98, when more than 11,000 km² of primary forest burned in Roraima (BARBOSA; FEARNSIDE, 1999).

Figure 3 - Annual precipitation maps modeled from TRMM 3B43 data for Roraima (municipalities in the state) and surrounding areas. The colored rectangles around the year on the maps represent the predominant climatic influence. Black = Normal years; yellow = La Niña years ; red = El Niño years (SILVA et al., 2015).

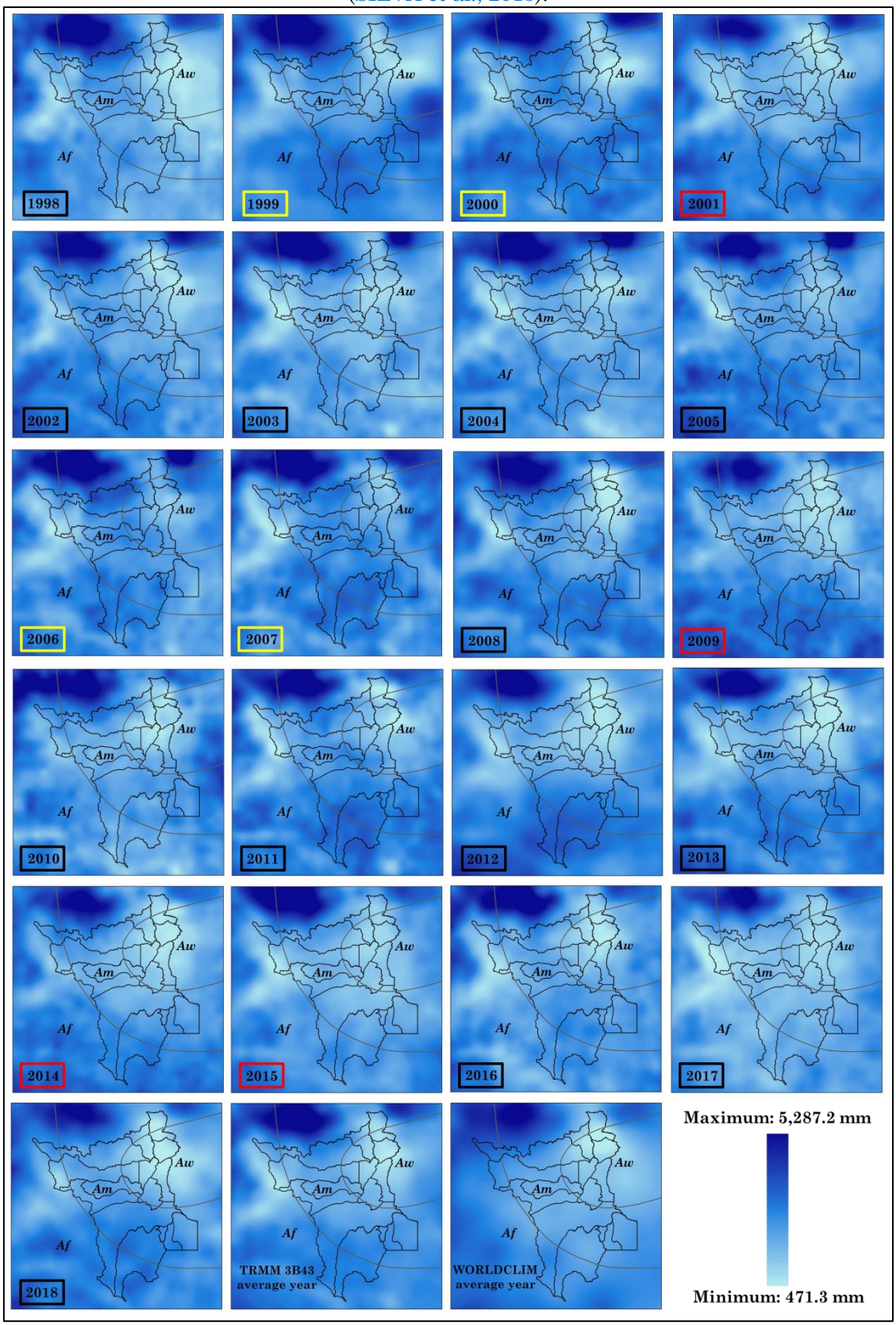

Organized by the authors, 2020.

Graph 4 - Annual distribution of rainfall in Roraima based on TRMM 3B43 data. The solid line represents the mean, the dashed line (M + SD) represents the mean plus the standard deviation of the period, and the dotted line (M-SD) represents the mean minus the standard deviation.

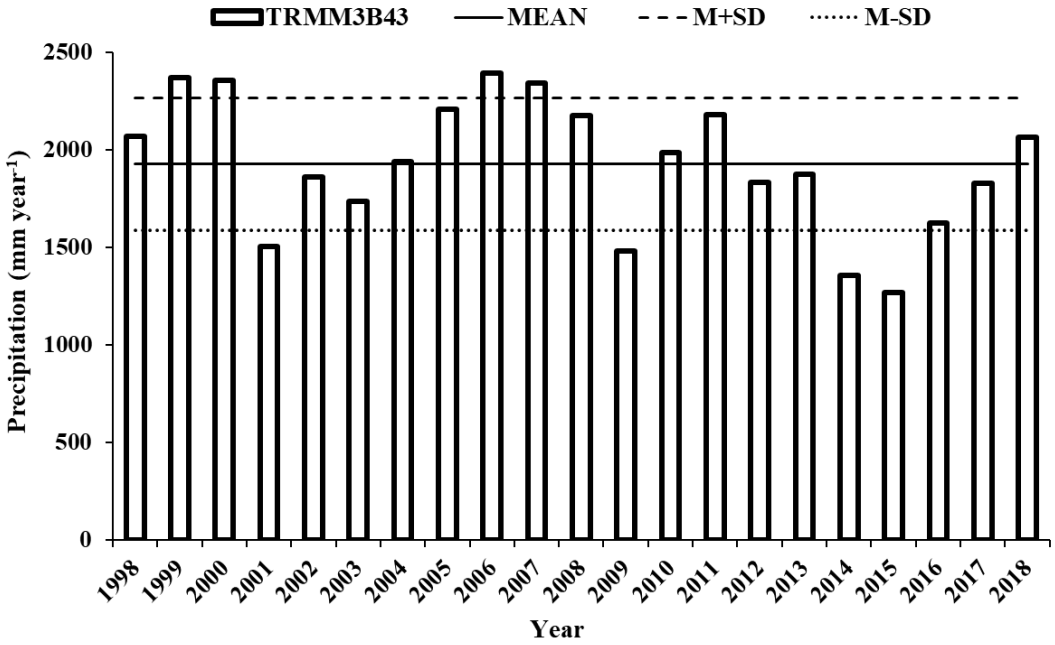

Organized by the authors, 2020.

The analysis of the parameters for ordinary kriging (curves of the theoretical models, nugget effect, range and sill), with reference to the annual maps, is presented in the supplementary material (Graph S1 and Table S1). The cross-validation carried out for the TRMM 3B43 annual maps indicated that these maps performed very well. The values of the coefficients of determination (adjusted R^2) for these maps were all above 92.4%. At least nine models (42.9%) had adjusted R^2 values above 97% (Table 5). After carrying out the above procedure, applying a simple regression model (n = 21) to the observed means (x) and estimated means (y), we obtained almost 100% agreement between the values (adjusted R^2 = 0.9986; p <0.0001).

Table 5 - Results of the cross-validation between the observed values (Mean_O) from TRMM and the values predicted by ordinary kriging (Mean_P) in each year at 75 reserved points (5.6%).

			Regression analysis			T test		
	Mean_O	**Mean_P**	**Std. dev.**	**$R^2_{Adj.}$**	***p***	**Std. dev**	**%**	***p***
1998	2380.8	2389.0	90.7	0.9704	<0.0000	523.7	22.0	0.9243
1999	2695.6	2706.8	98.2	0.9553	<0.0000	464.8	17.2	0.8824
2000	2666.0	2671.1	94.8	0.9621	<0.0000	490.0	18.4	0.9494
2001	2065.5	2078.1	103.8	0.9660	<0.0000	565.2	27.4	0.8920
2002	2341.0	2355.3	96.5	0.9738	<0.0000	595.5	25.4	0.8833
2003	2163.5	2174.0	85.0	0.9701	<0.0000	483.2	22.3	0.8950
2004	2330.8	2350.8	103.1	0.9597	<0.0000	511.4	21.9	0.8106
2005	2561.9	2562.6	86.4	0.9634	<0.0000	454.8	17.8	0.9917
2006	2599.4	2604.1	89.2	0.9640	<0.0000	471.5	18.1	0.9517
2007	2538.3	2562.4	90.4	0.9528	<0.0000	411.9	16.2	0.7209
2008	2649.9	2652.0	125.4	0.9242	<0.0000	461.0	17.4	0.9777
2009	2208.2	2203.3	121.2	0.9647	<0.0000	646.3	29.3	0.9633
2010	2460.7	2464.5	102.1	0.9564	<0.0000	489.9	19.9	0.9614

2011	2528.1	2516.8	93.9	0.9554	<0.0000	454.9	18.0	0.8792
2012	2390.7	2405.7	109.5	0.9706	<0.0000	640.3	26.8	0.8860
2013	2425.7	2436.6	112.3	0.9591	<0.0000	551.4	22.7	0.9036
2014	2074.7	2093.0	98.1	0.9775	<0.0000	652.8	31.5	0.8639
2015	1817.4	1822.5	90.1	0.9701	<0.0000	523.5	28.8	0.9527
2016	2135.0	2143.3	78.8	0.9778	<0.0000	532.3	24.9	0.9244
2017	2412.5	2416.8	74.2	0.9829	<0.0000	565.0	23.4	0.9626
2018	2607.1	2601.4	71.7	0.9819	<0.0000	539.4	20.7	0.9491

FINAL CONSIDERATIONS

The spatial and monthly rainfall patterns in Roraima are strongly influenced by the three existing climate types. The *Af* climate has the highest rainfall between the months of March and August, with the peak of precipitation in May. Due to its location close to the equator, this is the climate with the highest annual rainfall. On the other hand, *Am* and *Aw* have their rainfall peaks in June, with the rainy period extending from April to September. The *Aw* climate has the lowest annual precipitation and is restricted to savanna areas in the northeastern portion of the state. These facts are marked by the anticipation of annual rains in the southern part of the state, delaying their arrival for a few days or weeks in the northern and northeastern portions of the state.

In general, climatic phenomena represented by El Niño and La Niña years strongly control the climate in Roraima. The strong effect of these climatic anomalies is probably favored by the geographical position of the state, which has areas in both the northern and the southern hemispheres, influencing the state's three climate types. The maps modeled by the two databases were able to capture these climatic variations. In this case, regardless of the values attributed to each of the databases by the performance indicators, the modeled maps (both by TRMM and WORCLIM) are considered to be equally valid and useful for representing the precipitation variable in the state of Roraima and surrounding areas, considering the state's three climatic types.

Ordinary kriging was an effective method for geostatistical modeling and for creating precipitation maps for the state of Roraima and surrounding areas. This is important because these maps offer the opportunity to establish and organize climate models at the municipal level. However, it should be noted that this methodological sequence only serves as an alternative to the paucity of rain gauges in the region. The ideal solution would be to install a large physical network of rain gauges at regular intervals on the surface in order to improve the predictability of the spatial distribution of rainfall and to provide decision makers with high-quality local and regional information.

ACKNOWLEDGMENTS

We thank the State University of Roraima (UERR) for institutional and logistical support for conducting this study. R. I. Barbosa (Proc. 304204/2015-3) and P. M. Fearnside (311103/2015-4) received productivity grants from the National Council for Scientific and Technological Development (CNPq;).

REFERENCES

ALENCAR, A.; NEPSTAD, D.; DIAZ, M. D. V. Forest understory fire in the Brazilian Amazon in ENSO and non-ENSO years: area burned and committed carbon emissions. Earth Interactions, 10, 1–17. 2006. https://doi.org/10.1175/EI150.1

ALVARES, C. A.; STAPE, J. L.; SENTELHAS, P. C.; GONÇALVES, J. L. M.; SPAROVEK, G. Koppen's climate classification map for Brazil. **Meteorologische Zeitschrift**, V. 22, N. 6, p. 711–728. 2014. https://doi.org/10.1127/0941-2948/2013/0507

ALVARES, C. A.; GONÇALVES, J. L. M.; VIEIRA, S. R.; SILVA, C. R.; FRANCISCATTE, W. Spatial variability of physical and chemical attributes of some forest soils in southeastern of Brazil. **Scientia Agricola** (Piracicaba, Braz.) [online]. 2011, v. 68, n. 6. p. 697-705. 2011. https://doi.org/10.1590/S0103-90162011000600015

ARAGÃO, L. E. O. C.; MALHI, Y.; ROMAN-CUESTA, R. M.; SAATCHI, S.; ANDERSON, L. O.; SHIMABUKURO, Y. E. Spatial patterns and fire response of recent Amazonian droughts. Geophysical Research Letters, 34(7). 2007. https://doi.org/10.1029/2006GL028946

ARAGÃO, L. E. O. C; SHIMABUKURO, Y. E. The incidence of fire in Amazonian forests with implications for REDD. **Science**, v. 328, p. 1275-1278. 2010. https://doi.org/10.1126/science.1186925

AVITABILE, V.; HEROLD, M.; HEUVELINK, G. B. M.; LEWIS, S. L.; PHILLIPS, O. L.; ASNER, G. P.; ARMSTON, J.; ASHTON, P. S.; BANIN, L.; BAYOL, N.; et al. An integrated pan-tropical biomass map using multiple reference datasets. **Global Change Biology**, v. 22, n. 4, p. 1406–1420. 2016. https://doi.org/10.1111/gcb.13139

BACCINI, A.; GOETZ, S.; WALKER, W. et al. Estimated carbon dioxide emissions from tropical deforestation improved by carbon-density maps. **Nature Climate Change**, v. 2, p. 182–185. 2012. https://doi.org/10.1038/nclimate1354

BARBOSA, R. I.; XAUD, M. R.; SILVA, G. F. N.; CATTÂNEO, A. C. Forest Fires in Roraima, Brazilian Amazonia. **International Forest Fire News**, 28 (jan-jul), p. 51-56. 2003. Available at: https://pdfs.semanticscholar.org/903d/d1e0114c6cdefe67c0ebb4fe1b87e95fa22c.pdf. Accessed: 28 January 2020.

BARBOSA, R. I. Distribuição das chuvas em Roraima, p. 325-335. In: Barbosa, R.I.; Ferreira, E.F.G.; Castellon, E. G. (Eds.). **Homem, Ambiente e Ecologia no Estado de Roraima**. Instituto Nacional de Pesquisas da Amazônia (INPA), Manaus, Amazonas, Brasil. 1997.

BARBOSA, R. I.; FEARNSIDE, P. M. Incêndios na Amazônia: estimativa da emissão de gases de efeito estufa pela queima de diferentes ecossistemas de Roraima na passagem do evento — El Niño (1997/1998). **Acta Amazonica**, v. 29, p. 513-534. 1999. https://doi.org/10.1590/1809-43921999294534

BARNI, P. E.; FEARNSIDE, P. M.; GRAÇA, P. M. L. A. Desmatamento no Sul do Estado de Roraima: padrões de distribuição em função de Projetos de Assentamento do INCRA e da distância das principais rodovias (BR-174 e BR-210). **Acta Amazonica**, 42(2), 183-192. 2012. https://doi.org/10.1590/S0044-59672012000200000

BARNI, P. E.; PEREIRA, V. B.; MANZI, A. O.; BARBOSA, R. I. Deforestation and forest fires in Roraima and their relationship with phytoclimatic regions in the Northern Brazilian Amazon. **Environmental Management**, v. 55, n. 5, p. 1124-1138. 2015a. https://doi.org/10.1007/s00267-015-0447-7

BARNI, P. E.; FEARNSIDE, P. M.; GRAÇA, P. M. L. A. Simulating deforestation and carbon loss in Amazonia: impacts in Brazil's Roraima state from reconstructing Highway BR-319 (Manaus-Porto Velho). **Environmental Management**, v. 55, n. 2, p. 259-278. 2015b. https://doi.org/10.1016/j.foreco.2016.07.010

BARNI, P. E.; MANZI, A. O.; CONDÉ, T. M.; BARBOSA, R. I.; FEARNSIDE, P. M. Spatial distribution of forest biomass in Brazil's state of Roraima, northern Amazonia. **Forest Ecology and Management**, v. 377, p. 170–181. 2016. https://doi.org/10.1016/j.foreco.2016.07.010

BARNI, P. E.; SILVA, E. B. R.; SILVA, F. C. F. **Incêndios florestais de sub-bosque na zona de florestas úmidas do sul de Roraima: área atingida e biomassa morta**. In: Anais do Simpósio Brasileiro de Sensoriamento Remoto. Anais eletrônicos, Campinas, GALOÁ, p, 6280-6287. 2018. Available at: http://marte2.sid.inpe.br/col/sid.inpe.br/marte2/2017/10.27.15.44.12/doc/59747.pdf. Accessed: 18 July 2019.

BELLO-PINEDA, J.; HERNÁNDES-STEFANONI, J. L. Comparing the performance of two spatial interpolation methods for creating a digital bathymetric model of the Yucatan submerged platform. **Pan-American Journal of Aquatic Sciences**. v. 2, p. 247–254. 2007. https://www.researchgate.net/publication/252251187

BOHLING, G. Introduction to Geostatistics and Variograms Analysis. **Kansas Geological Survey**. 2005. Available at: <http://people.ku.edu/~gbohling/cpe940/>. Accessed: 8 April 2020.

BRANDO, P. M.; SOARES-FILHO, B.; RODRIGUES, L.; ASSUNÇÃO, A.; MORTON, D.; TUCHSCHNEIDER, D.; FERNANDES, E. C. M.; MACEDO, M. N.; OLIVEIRA, U.; COE, M. T. The gathering firestorm in southern Amazonia. **Science Advances**, v. 6, art. eaay1632. 2020. https://doi.org/10.1126/sciadv.aay1632

BRANDO, P. M.; BALCH, J. K.; NEPSTAD, D. C.; MORTON, D. C.; PUTZ, F. E.; COE, M. T.; SILVÉRIO, D.; MACEDO, M. N.; DAVIDSON, E. A.; NÓBREGA, C. C.; ALENCAR, A.; SOARES-FILHO, B. S.

Abrupt increases in Amazonian tree mortality due to drought–fire interactions. **Proceedings of the National Academy of Sciences USA**, v. 111, n. 17, p. 6347-6352. 2014. http://www.pnas.org/cgi/doi/10.1073/pnas.1305499111

CAMBARDELLA, C. A.; MOORMAN, T. B.; PARKIN, T. B.; KARLEN, D. L.; NOVAK, J. M.; TURCO, R. F.; KONOPKA, A. E. Field-scale variability of soil properties in central Iowa soils. **Soil Science Society of America Journal**, 58(5), p. 1501-1511. 1994. https://doi.org/10.2136/sssaj1994.03615995005800050033x

CAMMELLI, F.; ANGELSEN, A. Amazonian farmers' response to fire policies and climate change. **Ecological Economics**, 165, 106359. 2019. https://doi.org/10.1016/j.ecolecon.2019.106359

CASTRO, G. S. A.; MIRANDA, E. Desafios e oportunidades para o desenvolvimento agropecuário e social em Roraima. Embrapa Monitoramento por Satélite / Grupo de Inteligência Territorial Estratégica – GITE. Available at: https://www.embrapa.br/gite/projetos/regiaonorte/pdf/160801_GITE_REGIAO_NORTE_RORAIMA.pdf. Accessed: 2 May 2020. 2016.

CHEN, F.; LI, X. Evaluation of IMERG and TRMM 3B43 monthly precipitation products over mainland China. **Remote Sensing**, 8:472. 2016. https://doi.org/10.3390/rs8060472

DANCEY, C.; REIDY, J. **Estatística Sem Matemática para Psicologia**: Usando SPSS para Windows. Porto Alegre, Artmed. 2006.

FEARNSIDE, P. M. Amazon forest maintenance as a source of environmental services. **Anais da Academia Brasileira de Ciências**, v. 80, p. 101-114. 2008. https://doi.org/10.1590/S0001-37652008000100006

FEARNSIDE, P. M. Serviços ambientais provenientes de florestas intactas, degradadas e secundárias na Amazônia brasileira. In: PERES, C. A., GARDNER, T.A., BARLOW, J., VIEIRA, I. C. G. (Eds.), Conservação da Biodiversidade em Paisagens Antropizadas do Brasil. Editora da Universidade Federal do Paraná, Curitiba, Paraná, pp. 26-57. 2013.

FICK, S. E.; HIJMANS R. J. WorldClim 2: New 1 - km spatial resolution climate surfaces for global land areas. **International Journal of Climatology**, 37, 4302-4315. 2017. https://doi.org/10.1002/joc.5086

FIGUEIREDO FILHO, D. B.; SILVA JUNIOR, J. A. Desvendando os Mistérios do Coeficiente de Correlação de Pearson (r). **Revista Política Hoje**, Vol. 18, n. 1. p. 115-146. 2009. Available at: https://periodicos.ufpe.br/revistas/politicahoje/article/view/3852/3156. Accessed: 11 August 2019.

FONSECA-MORELLO, T.; RAMOS, R.; STEIL, L.; PARRY, L.; BARLOW, J.; MARKUSSON, N.; FERREIRA, A. Queimadas e incêndios florestais na Amazônia brasileira: por que as políticas públicas têm efeito limitado? **Ambiente & Sociedade**, v. XX, n. 4 n p. 19-40. 2017. https://doi.org/10.1590/1809-4422asoc0232r1v2042017

FONSECA, M. G.; ANDERSON, L. O.; ARAI, E.; SHIMABUKURO, Y. E.; XAUD, H. A. M.; XAUD, M. R.; MADANI, N.; WAGNER, F. H.; ARAGÃO, L. E. O. C. Climatic and anthropogenic drivers of northern Amazon fires during the 2015-2016 El Niño event. **Ecological Applications**, v. 27, n. 8, p. 2514-2527. 2017. https://doi.org/10.1002/eap.1628

GRIMM, A. M. The El Niño Impact on the Summer Monsoon in Brazil: Regional Processes versus Remote Influences. **American Meteorological Society**, 16, 263-280. 2003. https://doi.org/10.1175/1520-0442(2003)016<0263:TENIOT>2.0.CO;2

HIJMANS, R. J.; CAMERON, S. E.; PARRA, J. L.; JONES, P. G.; JARVIS, A. Very high resolution interpolated climate surfaces for global land areas. **International Journal of Climatology**, v.25, 1965-1978. 2005. https://doi.org/10.1002/joc.1276

HUFFMAN, G. J.; ADLER, R. F.; ARKIN, P.; CHANG, A.; FERRARO, R.; GRUBER, A.; JANOWIAK, J.; MCNAB, A.; RUDOLF, B.; SCHNEIDER, U. The Global Precipitation Climatology Project (GPCP) combined precipitation dataset. **Bulletin of the American Meteorological Society**, 78(1), 5–20. 1997. https://doi.org/10.1175/1520-0477(1997)078<0005:TGPCPG>2.0.CO;2

IBGE – INSTITUTO BRASILEIRO DE GEOGRAFIA E ESTATÍSTICA. Roraima: população. Available at: https://cidades.ibge.gov.br/brasil/rr/panorama. Accessed: 3 May 2020.

MACRITCHIE, K. **README**: Document for the Tropical Rainfall Measurement Mission (TRMM) Version 007. Goddard Earth Sciences Data and Information Services Center (GES DISC). 69 p. 2015.

MARENGO, J. A. Interannual variability of surface climate in the Amazon basin. **International Journal of Climatology**, 12, 853–863. 1992.

https://doi.org/10.1002/joc.3370120808
MEDINA, G.; ALMEIDA, C.; NOVAES, E.; GODAR, J.; POKORNY, B. Development conditions for family farming: lessons from Brazil. **World Development**, 74, 386-396. 2015. https://doi.org/10.1016/j.worlddev.2015.05.023
MELLO, Y. R.; OLIVEIRA, T. M. N. Análise Estatística e Geoestatística da Precipitação Média para o Município de Joinville (SC). **Revista Brasileira de Meteorologia**, v. 31, n. 2, 229-239. 2016. https://doi.org/10.1590/0102-778631220150040
MINISTÉRIO DO DESENVOLVIMENTO AGRÁRIO – MDA. PLANO TERRITORIAL DE DESENVOLVIMETO RURAL SUSTENTÁVEL: Propostas de Políticas Públicas para O Território Sul de Roraima. Available at: http://sit.mda.gov.br/download/ptdrs/ptdrs_qua_territorio091.pdf. Accessed: 2 May 2020. 2010.
MORTON, D. C.; LE PAGE, Y.; DE-FRIES, R.; COLLATZ, G. J.; HURTT, G. C. Understorey fire frequency and the fate of burned forests in southern Amazonia. **Philosophical Transactions of Royal Society for Biological Science B**, 368, 20120163. 2013. https://doi.org/10.1098/rstb.2012.0163
PASSOW M. J. TRMM Tropical rainfall measuring mission: Bringing remote sensing of precipitation into your classroom. TRMM: Trazendo o sensoriamento remoto de precipitação para sua sala de aula. **Terræ Didatica**, 6(1):03-08. Available at: <http://www.ige.unicamp.br/terraedidatica/>. Accessed: 15 April 2020. 2010
PRAKASH, S.; MITRA, A. K.; PAI, D. S.; AGHAKOUCHAK, A. From TRMM to GPM: How well can heavy rainfall be detected from space? **Advances in Water Resources**, 88, 1–7. 2016. https://doi.org/10.1016/j.advwatres.2015.11.008
R DEVELOPMENT CORE TEAM. R: A Language and Environment for Statistical Computing. R Foundation for Statistical Computing, Vienna, Austria. 2019. <http://www.r-project.org>
SILVA JR., C. H. L.; ANDERSON, L. O.; SILVA, A. L.; ALMEIDA, C. T.; DALAGNOL, R.; PLETSCH, M. A. J. S.; et al. Fire Responses to the 2010 and 2015/2016 Amazonian Droughts. **Frontiers in Earth Science**, v.7. 16p. 2019. https://doi.org/10.3389/feart.2019.00097
SILVA, C. V. J.; ARAGÃO, L. E. O. C.; BARLOW, J.; ESPÍRITO-SANTO, F.; YOUNG, P. J.; et al. Drought induced Amazonian wildfires instigate a decadal scale disruption of forest carbon dynamics. **Philosophical Transactions of Royal Society B**, 373: 20180043. 2018. https://doi.org/10.1098/rstb.2018.0043
SILVA, D. A.; SANDER, C.; ARAÚJO JR, A. C. R.; WANKLER, F. L. Análise dos ciclos de precipitação na região de Boa Vista – RR nos anos de 1910 a 2014. **Revista Geográfica Acadêmica**, v.9, 35-49, 2015. https://doi.org/10.18227/1678-7226rga.v9i2.3145
STAAL, A.; BERNARDO, M. F.; AGUIAR, A. P. D.; BOSMANS, J. H. C.; FETZER, I.; TUINENBURG, O. A. Feedback between drought and deforestation in the Amazon. Non-peer-reviewed EarthArXiv preprint. 2020. https://doi.org/10.31223/osf.io/8rq4n.
TERRAMZ: conhecimento compartilhado para gestão territorial local na Amazônia. Boa Vista, RR: Embrapa Roraima (Folder). Available at: http://ainfo.cnptia.embrapa.br/digital/bitstream/item/212385/1/TERRAMZ-Folder.pdf.. Accessed: 4 May 2020. 2020.
WOLFF, D. B.; MARKS, D. A.; AMITAI, E.; SILBERSTEIN, D. S.; FISHER, B. L.; TOKAY, A.; WANG, J.; PIPPITT, J. L. Ground Validation for the Tropical Rainfall Measuring Mission (TRMM). **American Meteorological Society**, v. 22, 365-380. 2005. https://doi.org/10.1175/JTECH1700.1
WU, C. R.; LIN, Y. F.; QIU, B. Impact of the Atlantic Multidecadal Oscillation on the Pacific North Equatorial Current bifurcation. **Scientific Reports**, 9, 2162. 2019. https://doi.org/10.1038/s41598-019-38479-w
YANG, Z.; HSU, K.; SOROOSHIAN, S.; XU, X.; BRAITHWAITE, D.; ZHANG, Y.; VERBIST, K. M. J. Merging high-resolution satellite-based precipitation fields and point-scale rain gauge measurements—A case study in Chile. **Journal of Geophysical Research: Atmospheres**, 122, 5267–5284. 2017. https://doi.org/10.1002/2016JD026177
XAUD, H. A. M.; MARTINS, F. S. R. V.; SANTOS, J. R. Tropical forest degradation by mega-fires in the northern Brazilian Amazon. Forest Ecology and Management, 294: 97-106. 2013. https://doi.org/10.1016/j.foreco.2012.11.036